Revista
Investigaciones
Geográficas

UNIVERSIDAD DE CHILE
FACULTAD DE ARQUITECTURA Y URBANISMO
DEPARTAMENTO DE GEOGRAFÍA

Lake ice phenology: a comparison between TSX and Sentinel-1 images using field data analysis in a maritime Antarctica region

Fenología del hielo lacustre: una comparación entre imágenes TSX y Sentinel-1 usando análisis de datos de campo en una región marítima de la Antártida

Historial del artículo

Received:
December 28, 2021
Revised:
June 11, 2022
Accepted:
June 14, 2022

Jorge Antônio Viel[a], Carina Petsch[b], Luiz Felipe Velho[c], Kátia Kellem da Rosa[d]

[a]Instituto Federal de Educação, Ciência e Tecnologia do Rio Grande do Sul - Campus Veranópolis, Brazil. Correo electrónico: ja-viel89@hotmail.com. ORCID: https://orcid.org/0000-0002-4139-9623
[b]Departamento de Geociências, Universidade Federal de Santa Maria, Brazil. Correo electrónico: carinapetsch@gmail.com. ORCID: https://orcid.org/0000-0002-1079-0080
[c]Instituto Federal de Educação, Ciência e Tecnologia do Rio Grande do Sul - Campus Porto Alegre, Brazil. Correo electrónico: lfvelho@gmail.com. ORCID: https://orcid.org/0000-0001-9543-7544
[d]Centro Polar e Climático, Universidade Federal do Rio Grande do Sul, Brazil. Correo electrónico: katiakellem@gmail.com. ORCID: https://orcid.org/0000-0003-0977-9658)

Keywords
Antarctica, cryosphere remote sensing, ice-free areas, surface ice cover.

Abstract

The monitoring of lake ice phenology in ice-free areas over time is relevant for understanding the impacts of global warming and extreme weather events in polar regions. The objectives of this work are: (i) to define backscatter values for ice-free and ice-covered surface water targets - which are supported by field data - as well as snow on lakes, from TerraSar-X (TSX) and Sentinel 1A - EW (S-1) images from the Fildes Peninsula, on Maritime Antarctica; (ii) to evaluate the relationship between backscatter and meteorological data; and (iii) to estimate the potentialities of TSX and S-1 for mapping lake phenology. These images were processed in SNAP, while the meteorological data were obtained from the Eduardo Frei Montalva Base. It was obtained a backscatter threshold of -32 dB to -21 dB for ice-free water in the lakes studied through the TSX image, although, for Sentinel-1, there was a range from -18 dB to -15 dB for ice-free water in the lakes. The TSX image is the most suitable for monitoring lake phenology, due to its spatial resolution, while the S-1 is limited to lakes of more than 10.000 m². It is recommended to consider meteorological conditions, especially wind, snow precipitation, and temperature changes, which represent significant changes in the backscatter values. The methodological recommendations regarding the use of TSX and S-1 imagery can be used for mapping lake ice cover and monitoring both ice break-up events and lake surface melt in glacial and periglacial environments.

Palabras clave
Antártida, áreas libres de hielo, cobertura de hielo, teledetección de la criosfera.

Resumen

El monitoreo a lo largo del tiempo de la dinámica fenológica de congelamiento de las superficies de los lagos en áreas libres de hielo es relevante para comprender los impactos del calentamiento mundial y los eventos climáticos extremos en las regiones polares. Los objetivos de este trabajo son: (I) establecer valores de retrodispersión para los blancos agua superficial libre de hielo y recubierta por hielo en lagos –con el soporte de datos de campo– utilizando las imágenes TerraSar-X (TSX) y Sentinel 1A - EW (S-1), teniendo como estudio de caso la península Fildes, Antárctica Marítima; (II) evaluar la relación entre los datos de retrodispersión y los datos meteorológicos; (III) evaluar las potencialidades de TSX y de S-1para el mapeo de la fenología de los lagos. El procesamiento de las imágenes SAR fue realizado en el SNAP y los datos meteorológicos fueron obtenidos en la Base Eduardo Frei Montalva. Se obtuvo el umbral de retrodispersión de -32 dB a -21 dB para el agua libre de hielo en los lagos estudiados en la imagen TSX, y para la Sentinel-1 hubo una variación de -18 dB a -15 dB para el agua libre de hielo de los lagos. La imagen TSX es la más adecuada para el monitoreo de la fenología de los lagos por su resolución espacial, mientras la S-1 se limita a los lagos con más de 10.000 m2. Es necesario tener en cuenta las condiciones meteorológicas, especialmente el viento, las precipitaciones de nieve y los cambios de temperatura, que representan alteraciones significativas en los valores de retrodispersión. Se puede utilizar las recomendaciones metodológicas referentes al uso de las imágenes TSX y S-1 para el mapeo de la cobertura de hielo en los lagos y el monitoreo de los eventos de quiebra de hielo y de derretimiento de la superficie de lagos en ambientes glaciales y periglaciales.

Cómo citar: Viel, J.A., Petsch, C., Velho, L.F. y da Rosa, K.K. (2022). Lake ice phenology: a comparison between TSX and Sentinel-1 images using field data analysis in a maritime Antarctica region. *Investigaciones Geográficas*, (63), 89-103. https://doi.org/10.5354/0719-5370.2022.67761

Introduction

Lakes and their ice regimes represent an important component of the cryosphere (Surdu et al., 2015). Freezing and thawing of lake ice has important consequences for physical, chemical, biological, and hydrological processes and influence local energy and water exchanges. The periodic lake formation and the decrease in ice cover over time, as a result of seasonal and interannual variations in climate, are called lake phenology (Kropáček et al., 2013; Šmejkalová et al., 2016).

Lake ice, break-up and thaw events are important for long-term monitoring and the detection of impacts related to global warming (Austin & Colman, 2007; Brown & Duguay, 2010; Cai et al. 2020; Duguay et al., 2002; Duguay et al., 2006; Duguay et al., 2015; Ke et al. 2013; Kouraev et al., 2007; Latifovic & Pouliot 2007; Miaomiao et al. 2019; Surdu et al. 2014;Vaughan et al. 2013; Zhang et al. 2020). However, there is limited understanding of the spatial patterns of lake ice phenology or about how these patterns are influenced by various climatic and geomorphic factors (O'Reilly et al., 2015), especially for Antarctica.

In this subject, satellite remote sensing has become a viable alternative to detect and monitor changes in ice cover in high-latitude lakes (Duguay et al., 2012; Latifovic & Pouliot, 2007; Murfitt & Brown 2017; Zhang & Pavelsky, 2019). SAR imagery has been used to characterize lake ice phenology for polar foreland at various spatial and temporal resolutions (Guo et al., 2018).

Ice lakes and open lakes SAR backscattering has been widely documented at various environments including North Slope of Alaska with ERS (Jeffries et al., 1994), the Canadian Subarctic (Duguay et al., 2002) with Radarsat C, the Arctic Alaskan Coastal Plain with Advanced Synthetic Aperture Radar (ASAR) Wide Swath and RADARSAT-2 ScanSAR (Surdu et al., 2015), and the Central Ontario with RADARSAT-2 data (Extra Wide mode and HH-polarized images) (Murfitt et al., 2018).

The TerraSAR-X images (HH polarization) allowed an unprecedented spatial and temporal detailing for proglacial lakes making it possible to map the ice cover lakes (Petsch et al., 2020). Antonova et al. (2016) monitored ice phenology in lakes of the Lena River delta using backscatter from TSX images. Sobiech & Dierking (2013) used TSX imagery with HH polarization to split ice and water fractions into lakes and river channels in the Lena River delta.

Recently, some investigators have demonstrated the potential of Sentinel-1 synthetic aperture radar (SAR) data for monitoring lake ice cover in Canada (Extra Wide (EW) mode, and HH polarization) (Duguay et al., 2015), in shallow lakes in northern Alaska (EW, and HH polarization) (Wakabayashi & Motohashi, 2018), in Fildes Peninsula, Maritime Antarctica foreland (Interferometric Wide mode, and HH polarization) (da Rosa et al., 2020). Moreover, in Antarctica, Dirscherl et al. (2021) devised the first automated method for mapping the extent of supraglacial lakes using S-1 imagery.

The increase in the availability of SAR data via the European Space Agency's (ESA) Copernicus Sentinel-1 A and B satellite platforms, and Copernicus/Alaskan Satellite Facility (ASF) data access utilities show the higher application for polar regions (Duguay et al., 2015). The Sentinel-1 satellite has 175 orbits per cycle and allows a more frequent revisit cycle (every 12 days) at southern latitudes. The evaluation of the performance of S-1 imagery for monitoring lake ice phenology in Antarctica can provide high-density time series and multisensory analysis. The validation of data obtained from SAR imagery is commonly performed by visual interpretation of optical images, such as Sentinel 2 (Murfitt & Duguay, 2020) MODIS (Murfitt & Duguay, 2020) Landsat (Geldsetzer & Sanden, 2013; Zhang et al., 2020), and/or field data (Zhang et al., 2020).

For the Antarctic environment, it is difficult to have field data collection on the passing day of the satellite or the coincidence of the passage of an optical sensor, considering the complexity and the costs of the logistics required to conduct fieldwork in Antarctica. In addition, frequent cloud cover limits the use of optical sensors. Given this, the objectives of this research are (i) to define backscatter values for ice-free water and ice and snow cover targets on the surface of glacial lakes of the Fildes Peninsula, at King George Island, for both TSX and S-1 images, which are supported by field photographs; (ii) to evaluate the relationship between backscatter values and meteorological data; and (iii) to estimate potentials and limitations of TSX and S-1 imagery for the mapping of lake phenology for the study area.

Materials and methods

Study area

The Fildes Peninsula (Fig. 1) is located in the southern part of King George Island – KGI - (62°08'S and 62°14'S; 59°02'W and 58°51'W), being bounded, to the northeast, by a small ice dome, the Collins Glacier (Fig. 1), at

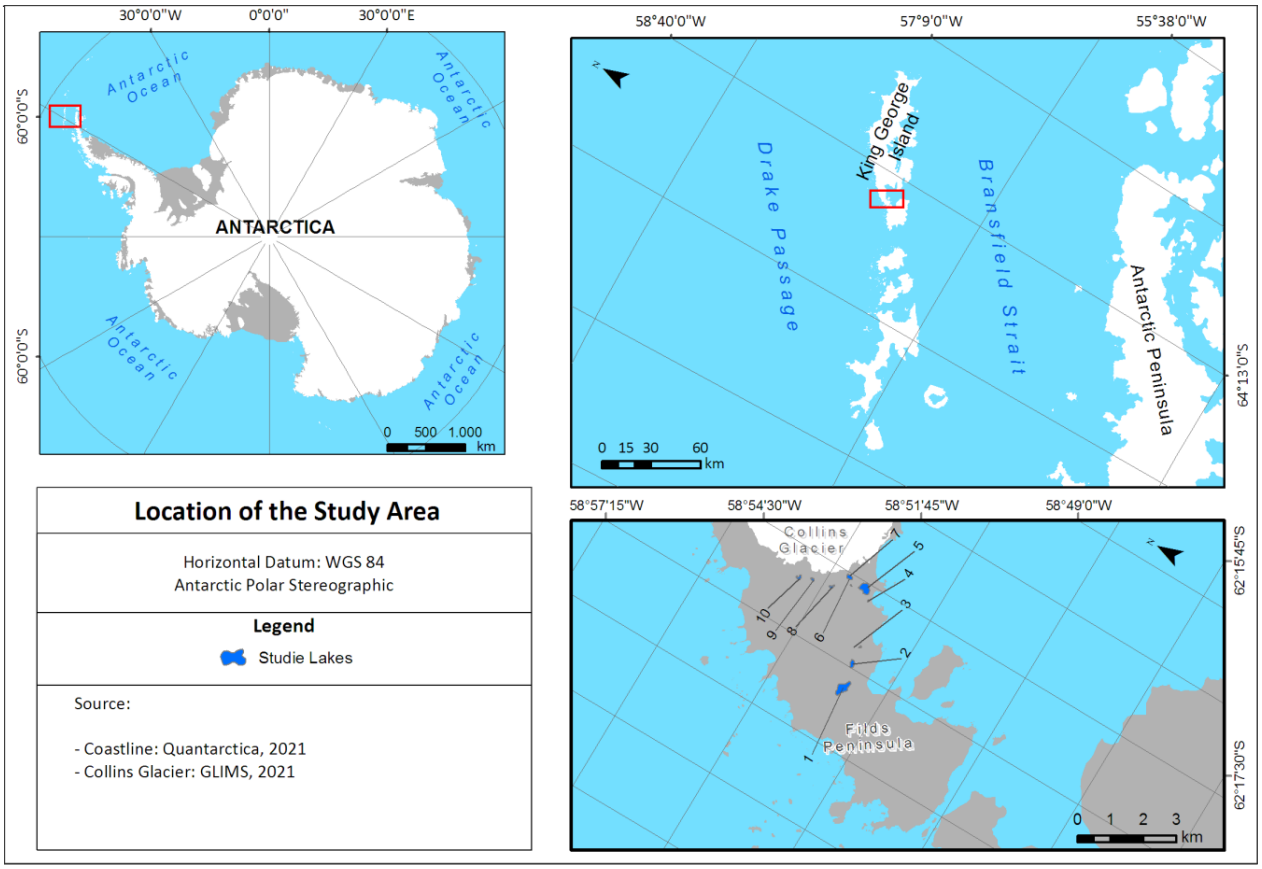

Figure 1. Location of lakes in Fildes Peninsula, King George Island and Antarctica.

approximately latitude 62°12'S and longitude 58°57'W. It has an area of 15 km² and its maximum elevation is 270 m. The ice displacement velocity in Collins Glacier is low, being estimated between 0.15 and 3.72 m a^{-1}, while, in the main King George Island ice dome, the maximum value reaches 112.1 m a^{-1} (Rückamp et al., 2010).

Annual mean air temperature is -2.8°C, with high weather variability (Ferron et al., 2004). The Bellinghausen Antarctic station on KGI had the highest annual mean temperature in the AP between 1981 and 2010. Pudełko et al. (2018) recorded changes in annual Positive Degree-Days from Bellingshausen, Jubany, and Ferraz stations on KGI from 1968 to 2010. Although Carrasco (2013) and Oliva et al. (2017) indicate a regional cooling trend since late 1990s and early 2000s. However, several studies have shown glacier retreat of Collins Glacier (Petsch et al. 2019ab; Rückamp et al. 2010) in the last decades.

The glacier retreat process in the northern part of the Fildes Peninsula reveals distinct environments, with melt flows coming from the glacier, giving rise to lakes and wetlands with two types of drainages: one facing the Drake Passage, and the other, facing Maxwell Bay. Petsch et al. (2019b) indicate the sequence of three proglacial lakes, which are connected and flow into Maxwell Bay. Vieira et al. (2015) point out that proglacial forms predominate in a small northern portion of the Fildes Peninsula, being associated with glacier activity and paraglacial forms that already have interference from other agents, such as wind, snow meltwater, and liquid precipitation. In the central portion, towards the south, the environments that predominate are periglacial, which includes processes of non-glacial erosion, mass movement on the slopes, wind, snow meltwater, and permafrost, as well as liquid precipitation (Vieira et al., 2015).

Processing the TSX and S-1 images

This research used Sentinel -1 (C band SAR) and TerraSAR-X (TSX) (X band SAR) data (Table 1). The Sentinel -1 was acquired in the Extra Wide (EW) swath mode and Level-1 Ground Range Detected (GRD) in either HH + HV and HH polarization with a pixel spacing of

Table 1
Data used in the analysis.

Sensor/ID	TSX	S-1
ID	TSX1_SAR__EEC_ SE___SM_S_ SRA_20150309T082300	S1A_EW_ GRDM_1SSH_ 20150309T233510
Data	2015-03-09	2015-03-09
Polarization	HH	HH
Passage	Downward	Downward
Band	X	C
Incidence angle	41.82° - 44.03°	18.41° - 45.99°
Mode	StripMap	Extra Wide
Spatial resolution (m)	3 x 3	40 x 40
Temporal resolution (days)	11	12

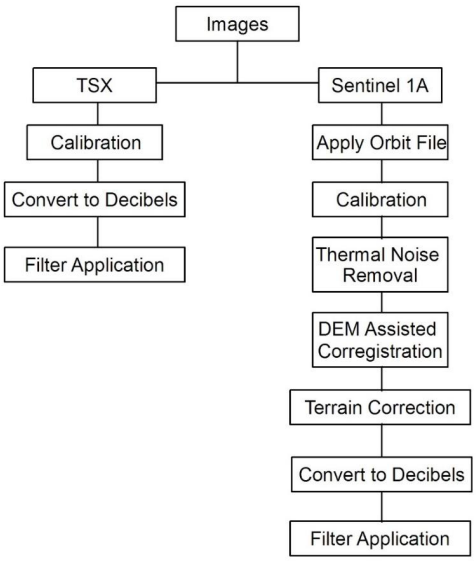

Figure 2. Workflow to obtain backscatter values.

40 m. The C-band of the S-1 image has a near incidence angle of 18.41° and a distant incidence angle of 45.99°. At the date of the fieldwork, there were no cloudless optical or S-1 IW images to be included in this study.

The TSX de 2015 is StripMap (a pixel spacing at 3 m), is Spatially Enhanced Product (SE) and Ellipsoid Enhanced Corrected (EEC). The 2015 TSX image has a near incidence angle of 41.82° and a distant incidence angle of 44.03°, being the downward passage. The image was downloaded from the European Space Agency (ESA) website.

A standard generic workflow to preprocess Copernicus Sentinel-1 GRD and TSX data is presented (Fig. 2). The workflow to preprocess Sl-1 GRD aims to apply Apply Orbit File, Thermal Noise Removal, Border Noise Removal, Calibration, Speckle Filtering, Range Doppler Terrain Correction, DEM-assisted, Conversion to a backscattering coefficient (in dB) in SNAP.

The vectoring of lakes and fieldwork

Field observations of the Fildes Peninsula lakes and their ice cover characteristics made during austral summer 2015 (February), which coincided with the acquisition of images, are used in support of the interpretation of the backscatter values. Ten lakes were selected for this study: three in the ice-marginal zone and seven in the no ice-marginal (periglacial) zone. The reasons that motivated this choice is the ice cover characteristics and environmental context of lakes are well known based on measurements obtained in February 2015. The lakes represent the main environments of the Fildes Peninsula, having already been described by Vieira et al. (2014) and Petsch et al. (2020).

The field photographs were recorded throughout the day, from 8 am to 4 pm, since the route was made without the aid of a motor vehicle. In the field, a Global Positioning System (GPS) equipment was used to capture the geographic coordinates of the target. The photographs of the lakes were taken from different angles and proximity in an attempt to contemplate their surroundings, also.

Lake vectors were extracted from visual interpretation (Wang et al., 2011) of February 28, 2008's QuickBird and 2018's Sentinel-2 images of the Fildes Peninsula ice-free area. QuickBird multispectral image (blue: 450–520 nm, green: 520–600 nm, red: 630–690 nm, NIR: 760–900 nm) (MS sensor) covering the study area and under clear sky conditions was acquired during the summer of 2008 (28, February). This image was taken at off-nadir angles (12–25- from nadir) with a pixel size of 2.4–2.8 m.

Sentinel-2 multispectral image (B2 (490 nm), B3 (560 nm), B4 (665 nm) and B8 (842 nm) (MSI sensor) covering the study area and under clear sky conditions was acquired during the summer of 2018. This image was a pixel size of 10 m. Image enhancement techniques (histogram analysis) were used to aid this interpretation. The vector

file of lakes was categorized numerically to assign a code to each lake (Gardelle et al., 2011).

The comparison with climatological data

We used the meteorological data (air temperature, wind and precipitation) provided by the station located at the Presidente Eduardo Frei Montalva base to analyze the influence of meteorological variables on the dynamics of freezing and thawing of the lake surface and on backscatter values. The SAR image response was related to both temperature and wind variables, seeking to identify the influence of these aspects on the results obtained. This steps to consider the effects of wind velocity in radar return and the dependence of the SAR geometry (Emery & Camps, 2017). The values found at the time of the image acquisition were analyzed, as well as the measures taken in the days before and after the radar image acquisition. It was analyzed the values obtained at the time of the image acquisition, as well as the ones from the days before and after the radar image achievement.

The obtaining of backscatter values

The vectors of the ten studied lakes are used to apply the SAR classification based on the backscattering thresholds that best represented the characteristics of the lakes on the fieldwork day (Table 3). Finally, it was extracted the mean and standard deviation statistical information for the set of studied places.

The methodology for obtaining the average backscattering coefficients for both ice-free water and ice and snow surface cover of the lakes was based on Murfitt et al. (2018). The backscatter coefficients adopted in this study were used to distinguish ice-free from the ice surface of each lake.

Results

Results show that mean σ° values at the ice lake cover of the -25.7 dB to TSX and of −16.5 dB to S-1, with a standard deviation of 2.6 and 0.94 dB, respectively (Table 2). And mean σ° values at the ice-free lake cover of the -17 dB to TSX and of -11.7 dB to S-1, with a standard deviation of 1.7 and 2.7 dB, respectively (Table 2).

Lakes 1 and 5 are the largest water bodies considered for this study (Figure 1). They are in different contexts: lake 1 occupies a central portion of the Fildes Peninsula and covers 91,719 m², while Lake 5 occupies an area of 81,009 m² and is located near the Collins Glacier, although it has no hydrological connection to the glacier. Lakes 3 and 4 have areas of 2,844 and 5,877 m², respectively, and they are located in the central portion, near Maxwell Bay, being protected from the Drake winds by the presence of the North Plateau. Lakes 8, 9 and 10 are located in areas that are directly influenced by the warmer north and west winds. Lake 7 occupies a more sheltered portion of the wind between the rocky portion and the advancing moraine of Collins Glacier, although it is connected to the glacier through a proglacial melt channel. Finally, lakes 1, 7 and 8 have a connection to other lakes via a liquid water transport channel, which may influence surface freezing and thawing.

Table 2
Mean backscatter coefficients of ice-free water and ice and snow cover on the surface of the studied lakes obtained through the S-1 e TSX images.

Image	Class	Average	Standard deviation
TSX	Ice-free Water	-25.7	2.62
	Ice and snow surface	-17.00	2.73
S-1	Ice-free Water	-16.5	0.94
	Ice and snow surface	-11.7	1.75

There is a visual correspondence between the floating ice cover and ice-free areas on the surface of the lake in the photographs and the TSX image. This correspondence is partially verified between the S-1 and TSX images (Table 3), except for lakes 7 and 8. In the S-1 image, lakes 7 and 8 are completely covered by ice and snow. Furthermore, it is not possible to completely distinguish the classes in the S-1 image for lakes with less than 10,000 m².

Figure 3 shows the media of pixel numbers for both ice and snow cover and ice-free surface classes for the group of the lakes. The ice-free surface area of the lake varies between 17% and 89% in the TSX image and between 17% and 100% in S-1 (Supplementary Table 1). In the S-1 image, most of the lakes (70%) have 0% ice-free pixels (open water) on their surfaces, which is not shown in the TSX image. The ice and snow cover class are identified in all lakes by both sensors, ranging from 15% to 82% for the TSX image and between 0% and 100% for the S-1 image.

The wind variable was observed to evaluate the differences in the backscatter measures in both images, regarding each class. Wind speed of 31 km/h is evident at the time of obtaining the TSX image, and 27 km/h at the time of obtaining the S-1 image (Table 1, Supplementary Table 2 and Figure 4). The wind speed reaches its maximum

Table 3

Comparisons between field photographs, TSX and S-1 images of the same date for the 10 lakes analyzed.

Lake	Field photographs	TSX Image	S-1 Image
1		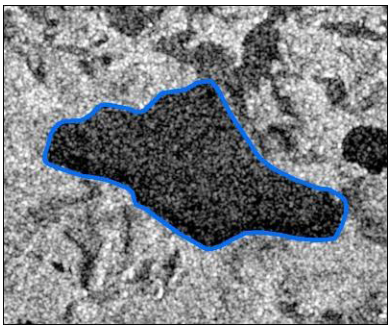	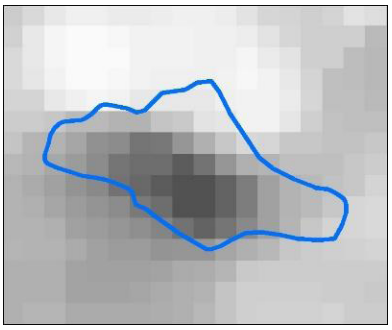
2		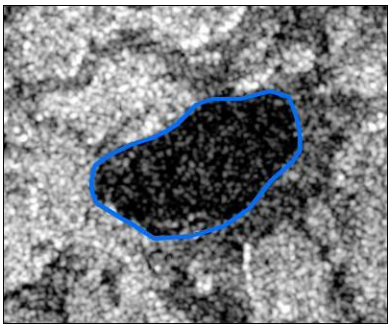	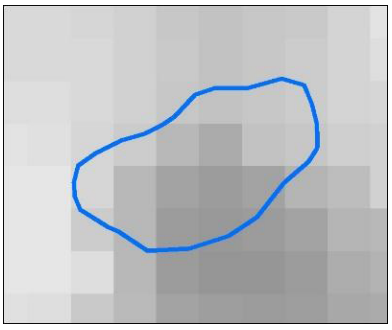
3		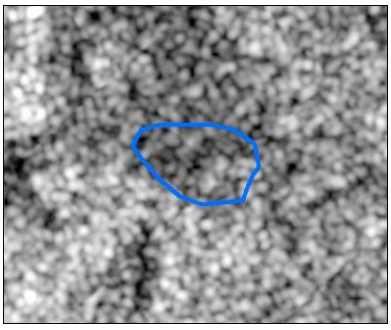	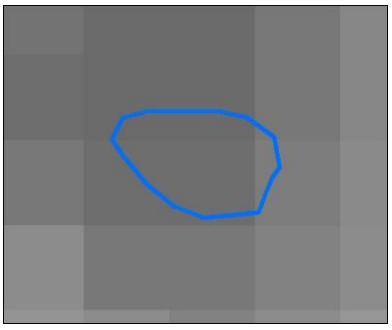

4		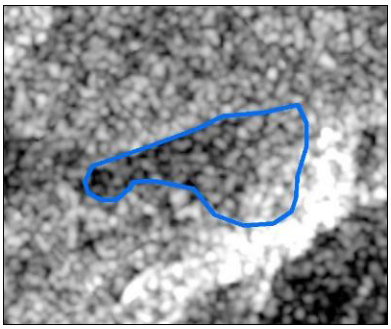	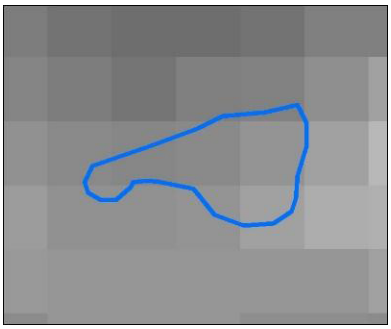
5		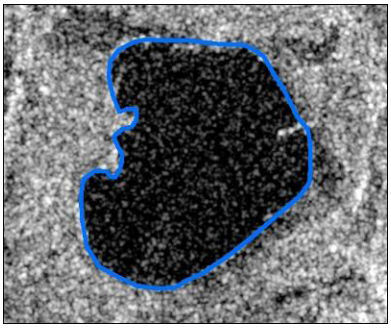	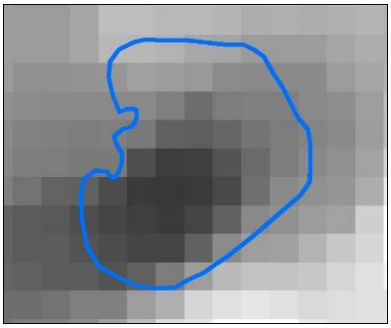
6		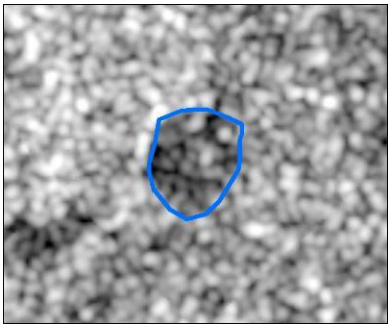	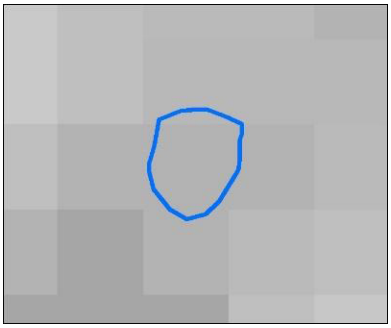

7		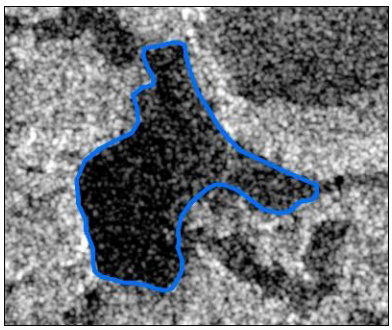	
8		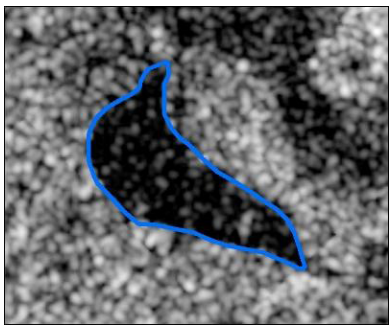	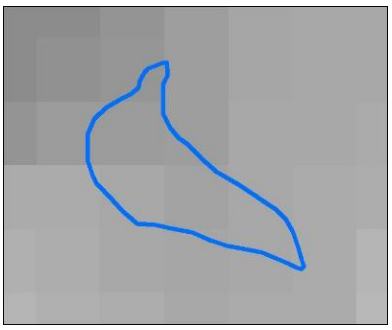
9		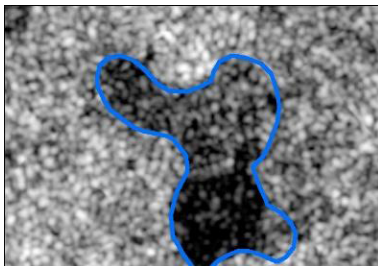	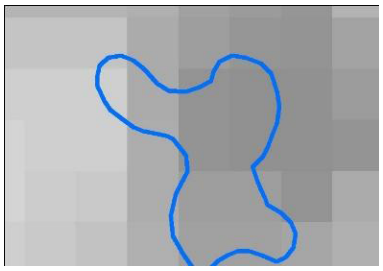
10		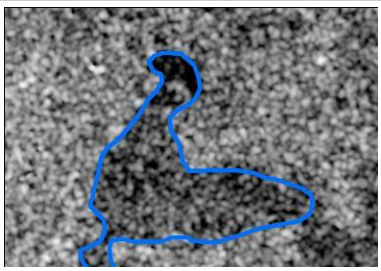	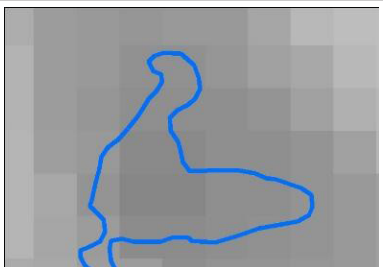

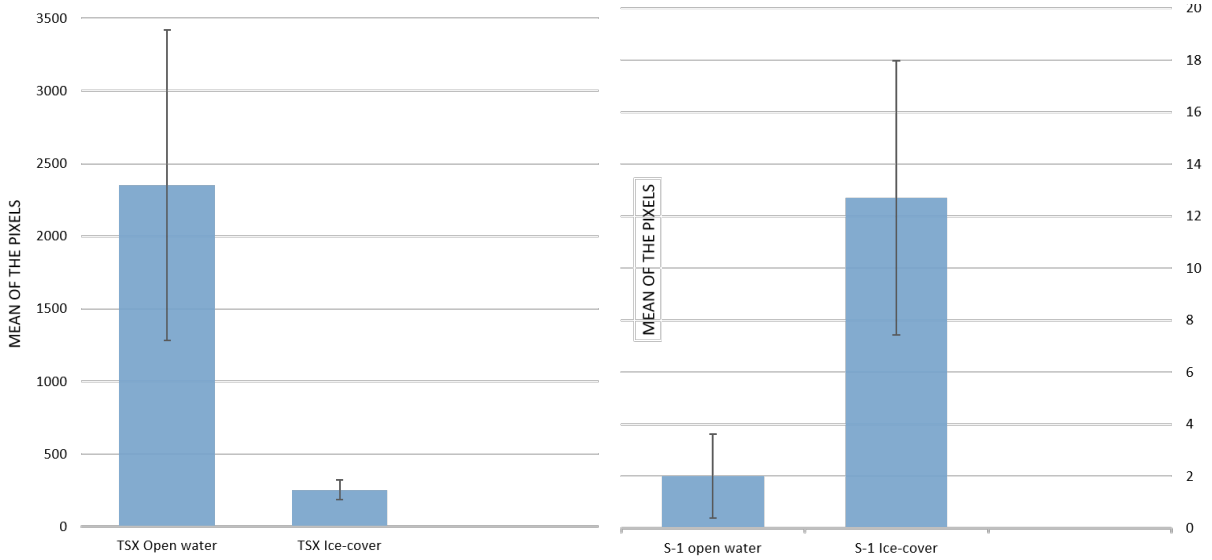

Figure 3. Comparisons between the number of pixels representing the surface coverage of lakes in the ice-free water and ice and snow surface in the images TSX and S-1. The vertical lines represent the standard deviation.

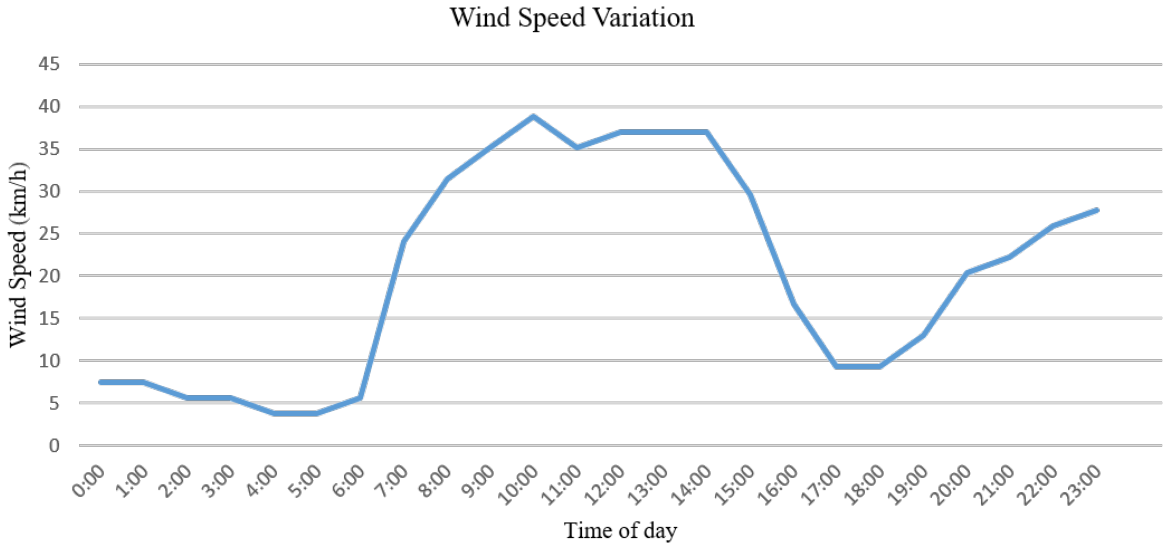

Figure 4. Wind speed variation (km/h) at 10 m height on March 9, 2015, in Fildes Peninsula.

values between 8 am and 4 pm, while the lowest speeds are seen between 0-6 am and 5-6 pm (Fig. 4). The lakes appear moderate dark in SAR images, which suggest of wind effect during the acquisition (e.g. Emery & Camps, 2017).

Considering the average air temperature in the last six-hour lapse (time of acquisition of TSX and S-1 images), it varied from -0.5 °C to 0.5 °C, while, in the 12-hour interval between the time of acquisition of both TSX and S1 images, the average air temperature varied from -0.5 ºC to 0.4 ºC. For the day, the average air temperature varied -0.2 °C and, for the month, 0.4 °C. March 7 and 8 had temperatures of 0.7 °C and 0.9 °C, respectively.

For the precipitation variable, the day of March 9, 2015, summed only 0.8 mm. However, the previous day had recorded 4.8 mm, which resulted in the snow-covered landscape of March 9. As far as fresh snow is concerned, it was recorded a value of 3 cm on March 8.

Discussion

Defining backscattering values between ice-covered free water and ice- and snow-covered surface

The open water lake cover is indicated by low mean σ° values (-25.7 dB to TSX and −16.5 dB to S-1, with a standard deviation of 2.6 and 0.94 dB, respectively). The backscattering of the EW mode Sentinel-1 agrees with Murfitt (2020). They presented a value of -21.72 dB with a standard deviation of 5.30 dB for surface lakes in the melting period using S-1 images (EW mode and HH polarization). Da Rosa et al. (2020) found values less than -17 dB for ice-free water in Fildes Peninsula lakes, by analyzing S-1 images in HH polarization and IW mode.

The authors analyzed Sentinel-1 images, Extra-Wide (IW) swath imaging mode, and HH polarization and found thresholds greater than -14 dB for the partially frozen class on the surface of the lakes. Da Rosa et al. (2020) obtained σ° values greater than -14 dB for frozen water (between -14 and -17 dB for the surface, with up to 60% of their frozen area). The average value found for lake ice and snow cover (-11.7 dB) in the S-1 image is in agreement with Wakabayashi & Motohashi (2018) and Rosa et al. (2020). Wakabayashi & Motohashi (2018) investigated the ice condition of shallow lakes in the Arctic region using the SAR data acquired by Sentinel-1 from 2015 to 2018 and confirmed that the C-band SAR data from Sentinel-1 could monitor the ice surface condition of shallow lakes. The authors to affirm that the backscattering threshold between floating and grounded ice was -14.8 to -16.8 dB depending on the incidence angle.

For the March 09, 2015 image, as noted in the photographs, the presence of snow may have interfered with the average recorded backscatter value of TSX (-17 dB) for the ice and snow surface. Antonova et al. (2016) point out that floating ice, formed in the Lena River delta, had a backscatter between -12 dB and -3.5 dB in TSX images. According to these authors, the snow cover in the frozen portion of the lake can melt and refreeze due to diurnal and nocturnal temperature variations, which are close to 0°C, configuring a situation, in which the backscatter can increase due to the roughness of this portion (Antonova et al., 2016). It was evidenced in this research since the meteorological data confirm the variation from -0.5 ºC to 0.4 ºC in the 12-hour lapse before the acquisition of the images.

Climatological variables

Considering the wind speed and direction (31 km/h at TSX (at 8:23 am) and 27 km/h at S-1 (at 11:35 pm) (Supplementary Table 2), it can be inferred that the lake surface may be influenced by winds in both images. Throughout the day, there were variations in wind intensity, as well as it was recorded bursts coming from all directions, which may have generated multiple effects on the backscatter recorded by both S-1 and TSX sensors, and on the position of the floating ice in lakes 2, 5, 8, and 9. Antonova et al. (2016) point out that, in windy conditions, the rougher water surface will cause more backscatter, making it more difficult to identify ice-free water.

It is also noteworthy that, for March 9, 2015, the predominant wind direction was southeast, which diverges from the conditions observed in March, in which north and west directions predominates. Petsch et al. (2020), by studying the lake phenology of the Fildes Peninsula with TSX imagery for the year 2011, point out that the change of wind direction from northwest and west to southeast freezes the lake surface afterward. In February, the northwest and west winds are more common, bringing precipitation, relative humidity, and cloud cover (Rakusa-Suszczewski et al., 2003). In lakes 8, 9, and 10, it can be seen that the nonaction of the moist and warm winds of the Drake Passage allowed the preservation of the frozen surface for a longer time.

Thus, it is highlighted that relief features are important in the analysis of wind influence. Regarding the freezing and thawing of lakes, Sobiech & Dierking (2013) highlight that, in coastal or mountainous environments, wind conditions change on local scales due to the altimetric conditions of the surroundings. This is the case of lakes 3, 4, and 6, which had the absence of floating ice since they are sheltered and do not suffer the direct action of the wind.

Considering that temperature is the main driver of lake ice variations (Šmejkalová et al., 2016), it is highlighted the importance of evaluating data before the passage of the sensors, although the effect of air temperature on lake ice is smaller during freezing than during fragmentation because freezing also depends on lake morphometry (depth, area, and volume), wind speed, and non-climatic variables, such as elevation or latitude (Surdu et al., 2015). The smaller, and possibly shallow, lakes (3, 4, 6, and 8) are influenced by their morphometric characteristics, responding quickly to air temperature changes (Surdu et al., 2015).

According to the studies of Watcham et al. (2011), lakes 1 and 5 (Fig. 4, Supplementary Table 1) are the largest and deepest lakes on the Fildes Peninsula, which may contribute to the development of physical properties of water favorable to maintaining the liquid surface. Variables, such as specific heat, make the water temperature not change at the same

rate as the environment. Lake 5 has a maximum depth of 14.7 m (Oaquim, 2017; Watcham et al., 2011), for instance. Large and deep lakes generally keep ice-free water for longer periods than smaller or shallower lakes at the same latitude and altitude (Šmejkalová et al., 2016). In addition, large lakes have a larger surface area, so they are more affected by wind action, which causes waves and facilitates ice break-up.

The day before the satellite pass, there was a significant precipitation event of liquid water and snow, which considerably altered the backscatter values on March 9, 2015, decreasing the contrast between ice lakes and their surroundings, as pointed out by Antonova et al. (2016). Considering the scenarios of changes in the pattern of both liquid precipitation and air temperatures, there are expected differences in backscatter signals in SAR images, which will affect small lakes mainly. Because small lakes warm up rapidly in summer and cool down rapidly in autumn, ice phenology may be more sensitive to climate change (Brown & Duguay, 2010; Zhang & Pvelski, 2019).

Inherent characteristics of each sensor: limitations and potential for monitoring lakes in the Maritime Antarctic

One factor that must be considered is the inherent characteristics of each SAR sensor, such as its spatial resolution and angle of incidence. These features contribute to the difference in values found in this study since radar images capture the difference in the position and geometry of targets. The backscattering of ice or water depends on the radar wavelength and polarization, as well as its incidence angle (Mäkynen et al., 2002). It is noteworthy that the X-band, for example, is more sensitive to wind speed and direction than images acquired at lower frequencies (Long et al., 1996).

In this sense, the higher incidence angles show changes in backscattering due to ice column characteristics (Atwood et al., 2015). Pogson et al. (2017), by analyzing sea ice with RadarSat-2 data, founded that open water generally has a high backscatter at a lower angle of incidence. The S-1 EW image shows less incidence angle variation in comparison to the TSX image. The angle of incidence, added to the roughness of the lake surface, caused by wind, may influence the underestimation of the number of pixels of ice-free water in the lakes studied.

The dependence on the observation geometry for the S-1 images can be decreased by normalizing the incidence angle to 30°, as recommended by Hillebrand et al. (2019). Both the relevance and evaluation of incidence angle normalization for SAR data are pointed out by Mladenova et al. (2013) and Topouzelis & Singha (2016), while Hillebrand et al. (2019) and Zhou et al. (2021) studied these features for S-1 sensor, specifically. In future studies, it could be evaluated to apply the same incidence angle value for both images, therefore normalizing the incidence angle issue.

It is pointed out that the detection of liquid water with radar imagery can also be difficult if the lake surface has snow, ice, and water (Hall et al., 1994). Thus, the highest pixel confusion results for S-1 images on distinguishing open water in lakes occurred mainly for smaller and shallower lakes, which highlights the limitation of using these images for studying phenology in lakes smaller than 10,000 m² in the study area, considering its spatial resolution. In addition, lakes 7 and 8, relatively larger, in terms of area, showed a different backscatter in comparison to the observed in the photos, presenting a predominance of snow cover, which may have a connection with the mixing of pixels (since advancing moraines, exposed rocks, and wetland areas, for example, represented targets that were covered by snow). However, given its spatial resolution limitation, the S-1 image in EW mode was shown to have the potential to detect ice-free liquid water cover for most of the lakes.

Concerning the wind sensitivity of SAR on water surfaces in general (discussed in the previous section), studies show that HH polarized data are less sensitive than VV polarized data (Partington et al., 2010; Sobiech & Dierking, 2013). As such, it was considered that HH polarized imagery is recommended for the separation of ice and water surfaces in Maritime Antarctica.

Because of what has been discussed, regarding the climatological and sensor characteristics, it is highlighted that the implementation of fixed thresholds possibly will not provide adequate results in the separation of both ice- and snow-covered surface and ice-free water for images from other dates or sensors, particularly for the TSX. Sobiech & Dierking (2013) point out that the thresholds need to be set according to the radar wavelength, polarization, and incidence angle, as well as the weather conditions of the acquisition date. As such, this study represents an initial effort to contribute to monitoring the ice phenology of Antarctic lakes, in the face of the small number of published papers on the topic (Da Rosa et al., 2020; Petsch et al., 2020). In addition, understanding ice lake phenology contributes to advancing other issues, such as the ecological processes on the presence of ice and its breakdown (Adrian et al., 1999; Hampton et al., 2017), and carbon balance (Adrian et al., 1999).

Final considerations

The backscattering values obtained through SAR were compared to the data and images collected in the field, which is innovative, given the difficulty of carrying out fieldwork on the Antarctic continent. There is a visual agreement in some lakes only, which is justified by the fact that the photographs were taken at different times of the day, as well as in different times of image acquisition, therefore with different floating ice positions and melting conditions. Although it is emphasized that field photographs were essential to ensure the improvement of the interpretation of the targets, since optical images are usually covered by clouds in the KGI portion, it is recommended that, in future works, the images should be taken at times close to the satellite passage.

It is concluded that it is not possible to delineate fixed thresholds for the detection and differentiation of ice cover from free water in the monitoring of ice lake phenology for the study area. It is recommended to perform tests with flexible threshold values for automatic target classification, seeking validation in optical imagery products or field photographs to aid in the interpretation of the environment. Additionally, weather conditions should be considered, especially wind, snow precipitation, and temperature changes, since, as observed in this study, the diurnal cycle of melting caused significant changes in backscatter values. It is indicated the analysis of the morphometric characteristics of the lakes' context, as well as the use of their depth data, which are scarce for Maritime Antarctica.

The S-1 imagery has great potential for monitoring ice lake phenology, as discussed in other research, but it is more effective in analyzing large areas of ice cover in lakes, which is not the case in the Maritime Antarctica region. Except for Lake 5, the S-1 images classified all lakes with predominant ice cover, diverging from the field acquired data. Undoubtedly, the TSX image presents an advantage in terms of spatial resolution, although the X-band is more affected by the wind variable, which is quite frequent in the study area. The TSX imagery was the most appropriate for the lakes of the study area.

References

Adrian, R., Walz, N., Hintze, T., Hoeg, S. & Rusche, R. (1999). Effects of ice duration on plankton succession during spring in a shallow polymictic lake. *Freshwater Biology*, *41*(3), 621-634. https://doi.org/10.1046/j.1365-2427.1999.00411.x

Antonova, S., Kääb, A., Heim, B., Langer, M., Boike, J. (2016): Principal Component Analysis of TerraSAR-X backscatter and coherence stacks one year (2012-2013) in the Lena River Delta, links to GeoTIFFs. PANGAEA, 169-191. https://doi.org/10.1594/PANGAEA.872142

Atwood, D.K., Gunn, G.E., Roussi, C., Wu, J., Duguay, C. & Sarabandi, K. (2015). Microwave Backscatter from Arctic Lake Ice and Polarimetric Implications. *Microwave Backscatter from Arctic Lake Ice and Polarimetric Implications*, *53*(11), 5972-5982. https://doi.org/10.1109/TGRS.2015.2429917

Austin J.A. & Colman S.M. (2007). Lake Superior summer water temperatures are increasing more rapidly than regional air temperatures: A positive ice-albedo feedback. *Geophysical Research Letters*, *34*(6). https://doi.org/10.1029/2006gl029021

Brown, L.C. & Duguay, C.R. (2010). The response and role of ice cover in lake-climate interactions. *Progress Physical Geography: Earth and Environment*, *34*(5), 671-704. https://doi.org/10.1177/0309133310375653

Cai, Y., Ke, C.Q., Yao, G. & Shen, X. (2020). MODIS-observed variations of lake ice phenology in Xinjiang, China. *Climatic Change*, *158*(3-4), 575-592. https://doi.org/10.1007/s10584-019-02623-2

Carrasco, J.F. (2013). Decadal changes in the near-surface air temperature in the western side of the Antarctic Peninsula. *Atmospheric and Climate Sciences*, *3*(3), 275-281. https://doi.org/10.4236/acs.2013.33029

da Rosa, C.N., Bremer, U.F., Pereira Filho, W. et al. (2020). Freezing and thawing of lakes on the Nelson and King George Islands, Antarctic, using Sentinel 1A synthetic aperture radar images. Environmental Monitoring and Assessment, 192 (559). https://doi.org/10.1007/s10661-020-08526-5

Dirscherl, M., Dietz, A.J., Kneisel, C. & Kuenzer, C. A. (2021). Novel Method for Automated Supraglacial Lake Mapping in Antarctica Using Sentinel-1 SAR Imagery and Deep Learning. *Remote Sensing*, *13*(2), 197. https://doi.org/10.3390/rs13020197

Duguay, C.R., Bernier, M., Gauthier, Y. & Kouraev, A. (2015). Remote Sensing of Lake and River Ice. *Remote Sensing of the Cryosphere*, (12), 273-306. https://doi.org/10.1002/9781118368909.ch12

Duguay, C., Brown, L., Kang, K.-K. & Kheyrollah Pour, H. (2012). The Arctic Lake ice, in "State of the climate in 2011". *Bulletin of the American Meteorological Society*, *93*(7), S152-S154. https://www.researchgate.net/publication/236173579_The_Arctic_Lake_ice_In_State_of_the_Climate_in_2011

Duguay, C. R., Prowse, T. D., Bonsal, B. R., Brown, R. D., Lacroix, M. P., & Ménard, P. (2006). Recent trends in Canadian lake ice cover. *Hydrological Processes*, *20*(4), 781-801. https://doi.org/10.1002/hyp.6131

Duguay, C.R., Pultz, T.J., Lafleur, P.M. & Drai, D. (2002). RADARSAT Backscatter Characteristics of Ice Growing on Shallow Subarctic Lakes, Churchill, Manitoba, Canada. *Hydrological Processes*, *16*(8), 1631-1644. https://doi.org/10.1002/hyp.1026

Emery, W. & Camps, A. (2017). Introduction to Satellite Remote Sensing. *Elsevier*, 291-453. https://doi.org/10.1016/B978-0-12-809254-5.00005-1

Ferron, F.A., Simões, J.C., Aquino, F.E. & Setzer, A.W. (2004). Air temperature time series for King George Island, Antarctica. *Pesquisa Antártica Brasileira*, (4), 155-169. https://www.researchgate.net/publication/37679700_Air_Temperature_Time_Series_for_King_George_Island_Antarctica

Gardelle, J., Arnaud, Y. & Berthier, E. (2011). Contrasted evolution of glacial lakes along the Hindu Kush Himalaya Mountain range between 1990 and 2009. *Global and Planetary Change*, *75*(1-2), 47-55. https://doi.org/10.1016/j.gloplacha.2010.10.003

Geldsetzer, T. & Sanden, J.J. (2013). Identification of polarimetric and nonpolarimetric C-band SAR parameters for application in the monitoring of lake ice freeze-up. *Canadian Journal of Remote Sensing*, *39*(3), 263-275. https://doi.org/10.5589/m13-033

Guo, L., Wu, Y., Zheng, H., Zhang, B., Li, J., Zhang, F. & Shen, Q. (2018). Uncertainty and Variation of Remotely Sensed Lake Ice Phenology across the Tibetan Plateau. *Remote Sensing*, *10*(10), 1534. https://doi.org/10.3390/rs10101534

Hall, D.K., Fagre, D.B., Klasner, F., Linebaugh, G. & Liston, G.E. (1994). Analysis of ERS 1 Synthetic Aperture Radar Data of Frozen Lakes in Northern Montana and Implications for Climate Studies. *Journal of Geophysical Research*, *99*(11), 22473-22482. https://doi.org/10.1029/94JC01391

Hampton, S.E, Galloway, A.W.E., Powers, S., Ozersky, T., Woo, K.H., Batt, R.D. Labou, S., O'Reilly, C.M., Sharma, S., Lottig, N., Stanley, E.H., North, R., Stockwell, J.D., Adrian, R., Weyhenmeyer, G., Arvola, L., Baulch, H., Bertani, I., Bowman, Jr. L. & Xenopoulos, M. (2017). Winter and summer comparison of biological, chemical, and physical conditions in seasonally ice-covered lakes. *Knowledge Network for Biocomplexity*, 136, 1 - 19. https://doi.org/10.5063/F12V2D1V

Hillebrand, L. F., da Rosa, C. N., Costi, J. & Bremer, U. F. (2019). Mapeamento do Gelo Marinho na Península Antártica com Imagens Sentinel 1A. *Anuário do Instituto de Geociências*, *42*(2), 59-71. https://doi.org/10.11137/2019_2_59_71

Jeffries, M.O., Morris, K., Weeks, W.F. & Wakabayashi, H. (1994). Structural and stratigraphic features and ERS 1 synthetic aperture radar backscatter characteristics of ice growing on shallow lakes in NW Alaska, winter 1991 - 1992. *Journal of Geophysical Research*, *99*(11), 22459 - 22471. https://doi.org/10.1029/94JC01479

Ke, C. Q., Tao, A. Q. & Jin, X. (2013). Variability in the ice phenology of Nam Co Lake in central Tibet from scanning multichannel microwave radiometer and special sensor microwave/imager: 1978 to 2013. *Journal of Applied Remote Sensing*, *7*(1), 073477. https://doi.org/10.1117/1.JRS.7.073477

Kouraev, A.V., Semovski, S.V., Shimaraev, M.N., Mognard, N.M., Legresy, B. & Remy, F. (2007). Observations of Lake Baikal ice from satellite altimetry and radiometry. *Remote Sensing Environment*, *108*(3), 240-253. https://doi.org/10.1016/j.rse.2006.11.010

Kropáček, J., Maussion, F., Chen, F., Hoerz, S. & Hochschild, V. (2013). Analysis of ice phenology of lakes on the Tibetan Plateau from MODIS data. *The Cryosphere*, *7*(1), 287-301. https://doi.org/10.5194/tc-7-287-2013

Latifovic, R. & Pouliot, D. (2007). Analysis of climate change impacts on lake ice phenology in Canada using the historical satellite data record. *Remote Sensing Environment*, *106*(4), 492-507. https://doi.org/10.1016/j.rse.2006.09.015

Long, D.G., Collyer, R.S. & Arnold, D.V. (1996). Dependence of the normalized radar cross section of water waves on Bragg wavelength–wind speed sensitivity. IEEE Trans. *IEEE Transactions on Geoscience and Remote Sensing*, *34*(3), 656-666. https://doi.org/10.1109/36.499745

Mäkynen, M.P., Manninen, A.T., Simila, M.H., Karvonen, J.A. & Hallikainen, M.T. (2002). Incidence angle dependence of the statistical properties of C-band HH-polarization backscattering signatures of the Baltic Sea ice. *IEEE Transactions on Geoscience and Remote Sensing*, *40*(12), 2593-2605. https://doi.org/10.1109/TGRS.2002.806991

Miaomiao, Q., Xiaojun, Y., Xiaofeng, L., Hongyu, D., Yongpeng, G. & Juan, L. (2019). Spatiotemporal characteristics of Qinghai Lake ice phenology between 2000 and 2016. *Journal of Geographical Sciences*, *29*(1),115-130. https://doi.org/10.1007/s11442-019-1587-0

Mladenova, I.E., Jackson T.J., Bindlish, R. & Hensley, S. (2013). Incidence angle normalization of radar backscatter data. *IEEE Transactions on Geoscience and Remote Sensing*, *51*(3), 1791-1804. https://doi.org/10.1109/TGRS.2012.2205264

Murfitt, J. & Brown, L. C. (2017). Lake ice and temperature trends for Ontario and Manitoba: 2001 to 2014. *Hydrological Processes*, *31*(21), 3596 - 3609. https://doi.org/10.1002/hyp.11295

Murfitt, J., Brown, L.C. & Howell, S.E.L. (2018). Evaluating RADARSAT-2 for the Monitoring of Lake Ice Phenology Events in Mid-Latitudes. *Remote Sensing*, *10*(10), 1 - 26. https://doi.org/10.3390/rs10101641

Murfitt, J. & Duguay, C. R. (2020). Assessing the Performance of Methods for Monitoring Ice Phenology of the World's Largest High Arctic Lake Using High-Density Time Series Analysis of Sentinel-1 Data. *Remote Sensing*,*12*(3),1 - 25. https://doi.org/10.3390/rs12030382

Oaquim, A.B. (2017). *Assembléias de diatomáceas em testemunho sedimentar do lago Proglacial Glubokoe Deepe, Península Fildes, Ilha Rei George, Antártica, como indicadores de variabilidade climática regional* [Dissertação para obter o título de mestre em Geociências com ênfase em geoquímica, Universidade Federal Fluminense, Rio de Janeiro, Brasil]. https://www.lume.ufrgs.br/handle/10183/32700.

Oliva, M., Antoniades, D., Giralt, S., Granados, I., Pla-Rabes, S., Toro, M., Liu E.J., Sanjurjo, J. & Vieira, G. (2017). The Holocene deglaciation of the Byers Peninsula (Livingston Island, Antarctica) based on the dating of lake sedimentary records. *Geomorphology*, *261*, 89-102. https://doi.org/10.1016/j.geomorph.2016.02.029

O'Reilly, C.M., Sharma, S., Gray, D.K., Hampton, S.E., Read, J.S., Rowley, R.J. et al. (2015). Rapid and highly variable warming of lake surface waters around the globe. *Geophysical Research Letter*, *42*(24), 1 - 9. https://doi.org/10.1002/2015GL066235

Petsch, C., Costa, R. M., Rosa, K. K., Vieira, R. & Simões, J. C. (2019a). Identificação e mapeamento em mesoescala da zona proglacial da Geleira Collins, Ilha Rei George, Antártica. *Quaternary and Environmental Geosciences*, *10*(1-2), 18-39. https://doi.org/10.5380/abequa.v10i1.60643

Petsch, C., Costa, R. M., Rosa, K. K. da., Vieira, R. & Simões, J. C. (2020). Geomorfologia glacial e contexto paleoglaciológico da Península Fildes, Ilha Rei George, Antártica. *Revista Brasileira de Geomorfologia*, *20*(4), 795-809. https://doi.org/10.20502/rbg.v20i4.1480

Petsch, C., Sotille, M. E., Costa, R. M., Rosa, K. K. & Simões, J. C. (2019b). Cambios climáticos y aumento de la vegetación en la Península Fildes, Antártica. *Investigaciones Geográficas*, (57), 18-31. https://doi.org/10.5354/0719-5370.2019.52147

Pogson, L., Geldsetzer, T., Buehner, M., Carrieres, T., Ross, M. & Scott, A. K. (2017). Collecting Empirically Derived SAR Characteristic Values over One Year of Sea Ice Environments for Use in Data Assimilation. *Monthly Weather Review*, *145*(1), 323-334. https://doi.org/10.1175/MWR-D-16-0110.1

Partington, K. C. Flach, J. D. Barber, D. Isleifson, D. Meadows, P. J. & Verlaan, P. (2010). Dual-Polarization C-Band Radar Observations of Sea Ice in the Amundsen Gulf. IEEE Transactions on Geoscience and Remote Sensing, 48(6), 2685-2691. https://doi.org/10.1109/TGRS.2009.2039577

Pudełko, R., Angiel, P., Potocki, M., Jędrejek, A. & Kozak, M. (2018). Fluctuation of Glacial Retreat Rates in the Eastern Part of Warszawa Icefield, King George Island, Antarctica, 1979–2018. *Remote Sensing*, *10*(6), 1 - 25. https://doi.org/10.3390/rs10060892

Rakusa−Suszczewski, S. (2003). Functioning of the geoecosystem for the west side of Admiralty Bay (King George Island, Antarctica): Outline of research at Arctowski Station. *Ocean and Polar Research*, *25*(4), 653-662. https://doi.org/10.4217/OPR.2003.25.4.653

Rückamp, M., Blindow, N., Suckro, S., Braun, M., & Humbert, A. (2010). Dynamics of the ice cap on King George Island, Antarctica: field measurements and numerical simulations. Annals of Glaciology, 51(55). https://doi.org 10.3189/172756410791392817.

Šmejkalová, T., Edwards, M. E. & Dash, J. (2016). Arctic lakes show strong decadal trend in earlier spring ice-out. *Scientific Reports*, (6), 1 – 8. https://doi.org/10.1038/srep38449

Sobiech, J. & Dierking, W. (2013). Observing lake- and river-ice decay with SAR: Advantages and limitations of the unsupervised k-means classification approach. *Annals of Glaciology*, *54*(62), 65-72. https://doi.org/10.3189/2013AoG62A037

Surdu, C. M., Duguay, C. R., Brown, L. C. & Prieto, F. D. (2014). Response of ice cover on shallow lakes of the North Slope of Alaska to contemporary climate conditions (1950–2011): radar remote-sensing and numerical modeling data analysis. *The Cryosphere*, *8*(1), 167-180. https://doi.org/10.5194/tc-8-167-2014

Surdu, C.M., Duguay, C.R., Pour, H.K. & Brown, L.C. (2015). Ice Freeze-up and Break-up Detection of Shallow Lakes in Northern Alaska with Spaceborne SAR. *Remote Sensing*, *7*(5), 6133-6159. https://doi.org/10.3390/rs70506133

Topouzelis, K. & Singha, S. (2016). Incidence angle normalization of wide swath SAR data for oceanographic applications. *Open Geosciences*, *8*(1), 450-464. https://doi.org/10.1515/geo-2016-0029

Vaughan, D. G., Comiso, J. C., Allison, I. et al. (2013). Observations: Cryosphere. In T.F. Stocker, D. Qin, G.K. Plattner et al., *Climate Change 2013: The Physical Science Basis. Contribution of Working Group I to the Fifth Assessment Report of the Intergovernmental Panel on Climate Change*. Cambridge University Press.

Vieira, G.; Mora, C.; Pina, P.; Schaefer. C. E. R. (2014). A proxy for snow cover and winter ground surface cooling: Mapping Usnea sp. communities using high resolution remote sensing imagery (Maritime Antarctica). Geomorphology, 225, 69-75.

Wakabayashi, H. & Motohashi, K. (2018). *Monitoring Freezing and Thawing of Shallow Lakes in Northern Alaska Using Sentinel-1 Data* [Trabalho apresentado no International Geoscience and Remote Sensing Symposium, Valencia, Espanha].

Wang, W., Yao, T. & Yang, X. (2011). Variations of glacial lakes and glaciers in the Boshula mountain range, southeast Tibet, from the 1970s to 2009. *Annals Of Glaciology*, *52*(58), 9-17. https://doi.org/10.3189/172756411797252347

Watcham, E.P., Bentley, M.J., Hodgson, D.A., Roberts, S.J., Fretwell, P.T., Lloyd, J.M., Larter, R.D., Whitehouse, P.L., Leng, M.J., Monien, P. & Moreton, S.G. (2011). A new Holocene relative sea level curve for the South Shetland Islands, Antarctica. *Quaternary Science Reviews*, *30*(21-22), 3152- 3170. https://doi.org/10.1016/j.quascirev.2011.07.021

Zhang, S. & Pavelsky, T.M. (2019). Remote Sensing of Lake Ice Phenology across a Range of Lakes Sizes, ME, USA. *Remote Sensing*, *11*(14), 1 -13. https://doi.org/10.3390/rs11141718

Zhang, S., Pavelsky, T. M., Arp, C. D. & Yang, X. (2020). Remote sensing of lake ice phenology in Alaska. *Environmental Research Letters*, *16*(6), 1 - 12. https://doi.org/10.1088/1748-9326/abf965

Zhou, C., Liu, Y. & Zheng, L. (2021). Satellite-derived dry-snow line as an indicator of the local climate on the Antarctic Peninsula. *Journal of Glaciology*, *68*(267), 1–11. https://doi.org/10.1017/jog.2021.72